Article

Effectiveness of Hybrid Geosynthetic Systems in Controlling Differential Heave in Flexible Pavements over Expansive Soils

Mir Md. Tamim [1] , Debakanta Mishra [2] and Bhaskar C. S. Chittoori [3,*]

[1] Idaho Transportation Department, Boise, ID 83714, USA; mir.tamim@itd.idaho.gov
[2] School of Civil and Environmental Engineering, Oklahoma State University, Stillwater, OK 74078, USA; deb.mishra@okstate.edu
[3] Department of Civil Engineering, Boise State University, Boise, ID 83725, USA
[*] Correspondence: bhaskarchittoori@boisestate.edu

Abstract: The challenge of maintaining ride quality and serviceability in flexible pavements built over expansive soil deposits remains a critical concern for transportation agencies. These expansive subgrades exhibit swell-shrink behavior in response to moisture fluctuations, leading to differential heaving and subsequent costly maintenance. This paper explores the effectiveness of a Hybrid Geosynthetic Reinforcement System (HGRS)—a composite of geocell and geogrid—as a targeted mitigation strategy for differential heaving induced by expansive soils. A large-scale box test was designed to simulate a flexible pavement section, consisting solely of a base course layer and the underlying expansive subgrade. Four test conditions were investigated: an unreinforced control, a geocell-reinforced section, a geogrid-reinforced section, and an HGRS-reinforced section. Vertical displacements on the surface of the base course layer were longitudinally monitored and compared against the control. The results reveal that the use of geosynthetic reinforcements, and HGRS in particular, significantly mitigates both maximum surficial heave and differential swelling. Among the systems tested, flexible pavements featuring HGRS demonstrated the most effective performance in alleviating the challenges posed by expansive soil deposits.

Keywords: expansive soils; geosynthetics; hybrid system; geocells; geogrids; large-scale box tests; differential heave

1. Introduction

Flexible pavements constructed over expansive subgrades are susceptible to upward heaving and cracking, phenomena attributed to the swelling behavior of the underlying soil layers [1]. These problematic soils often contain the clay mineral 'Montmorillonite', known for its substantial volume changes with fluctuations in moisture content [2]. Expansive soils are widespread in the United States, often rendering them unavoidable during road construction projects [3]. The economic implications are significant; between 1973 and 2012, the annual cost of damages attributed to expansive soils in the United States rose by a factor of 6.8 [4]. Lightly loaded structures, such as pavements, are particularly vulnerable as their own weight is insufficient to counterbalance the expansive forces from the subgrade, necessitating increased budget allocation for repairs [5].

Various remedial strategies, including chemical stabilization, have been tried with varying degrees of success [1,6,7]. Chemical stabilization is a common approach, but its effectiveness is often compromised by the problem's inherent complexity and the high costs associated with implementation [7,8]. For instance, sections of US Highway 95 near the Idaho-Oregon border have experienced persistent issues despite multiple rehabilitation efforts [4,9]. Research from Boise State University demonstrated that conventional chemical stabilization methods were not suitable due to the expansive subgrade soils' depth and high sulfate contents, which limit the use of calcium-based stabilization [9–11].

To address these limitations, this study introduces the Hybrid Geosynthetic Reinforcement System (HGRS)—a composite of geocell and geogrid materials—as a novel mitigation strategy [9]. A large-scale box test was employed to simulate a pavement section, which included a base course layer and the expansive subgrade below. The study examined four scenarios: an unreinforced control, a geocell-reinforced section, a geogrid-reinforced section, and an HGRS-reinforced section. Vertical displacements on the surface of the base course were longitudinally monitored and compared [9]. This paper aims to present the results, highlighting the efficacy of HGRS in mitigating the challenges posed by expansive soil deposits.

2. Background

Soil stabilization presents a challenging yet critical aspect in civil engineering, particularly concerning expansive soils that undergo volumetric changes due to moisture variations. Among the multiple solutions explored, geosynthetics have shown considerable promise in mitigating some of these challenges. Geogrids, one such geosynthetic material, have gained popularity for their reinforcing mechanism [12]. Comprising a uniformly distributed array of apertures between longitudinal and transverse tension-bearing elements, geogrids reinforce soil through lateral frictional resistance, enhanced bearing capacity, and a membrane effect [13,14]. Their applications are broad and have proven successful in providing construction platforms over weak subgrades and reinforcing pavements [15–20]. However, the membrane effect often necessitates significant deformation [21].

Following the introduction of geogrids, geocells also emerged as a viable solution for soil stabilization. Developed initially in the 1970s for lateral confinement in soils with low bearing capacity, geocells have found extended applications in reinforcing pavement bases [22,23]. The geocell system's reinforcing mechanism includes stresses within the cells, passive resistance in adjacent cells, and hoop stresses around cell walls [24–27]. While experimental studies have demonstrated geocells' ability to significantly increase soil's bearing capacity [28–32], the existing literature provides insufficient evidence for their efficacy in mitigating expansive soil-induced swell pressures.

Further enhancing the potential of geosynthetics in soil stabilization, Stienberg highlighted the utility of geomembranes in controlling soil swelling [33]. Other researchers like Vessely and Wu have demonstrated the effectiveness of geotextiles in stabilizing problematic soils [34], and Zornberg et al. have further corroborated this by showing that geotextiles could mitigate swelling-induced cracks in pavements constructed over expansive soils [35].

With advancements in geosynthetics, a new focus is the Hybrid Geosynthetic Reinforcement System (HGRS), which combines the strengths of both geocells and geogrids [36]. Figure 1 illustrates the combined effect of HGRS. In the figure, orange, purple, blue, red, and sky blue arrows represent the confinement within the cell, frictional resistance within the cell wall, passive earth resistance due to adjacent cells, membrane effect, and lateral resistance, respectively. Initial research in applications like railroads and embankments has shown that the HGRS improves bearing capacity and mitigates soil swelling, indicating a promising future for this composite system [27,37].

This research aims to delve into the application and effectiveness of HGRS in mitigating challenges associated with expansive soils, thereby addressing a gap in the current literature.
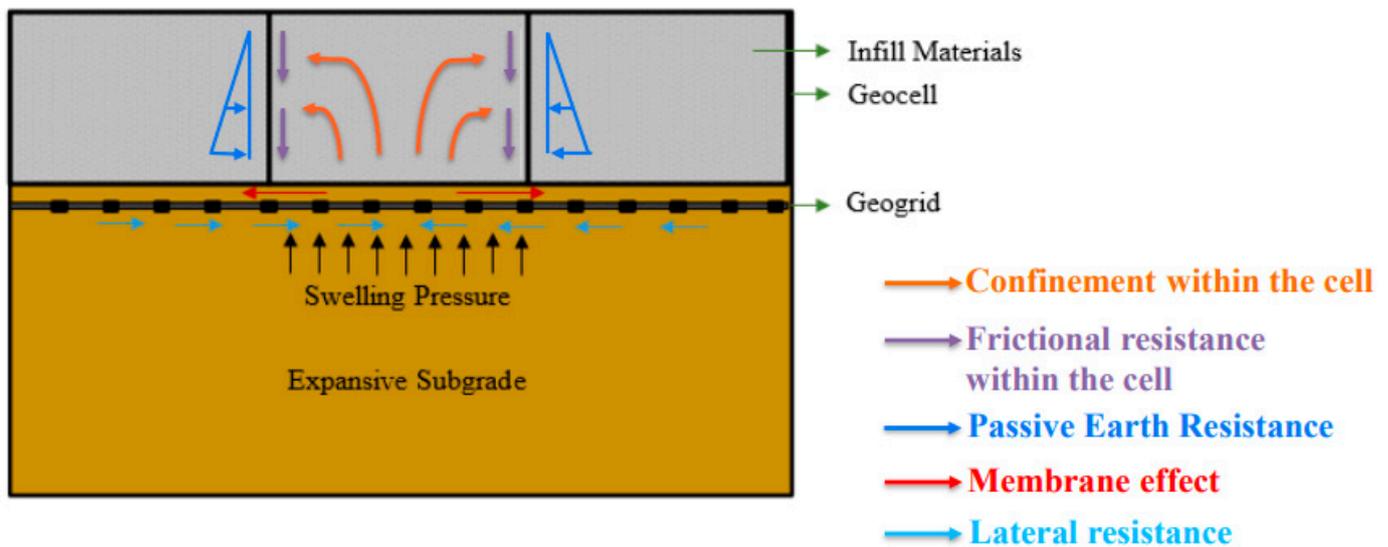
Figure 1. Reinforcing mechanism of HGRS.

3. Experimental Program

As previously noted, conventional loading configurations for flexible pavements are ill-suited for conditions involving swell pressures arising from expansive soils. In standard scenarios, loads are generally applied at the pavement surface and dissipate progressively through underlying layers. However, the presence of expansive soils introduces an inverted loading condition, wherein upward pressures from swelling soils must be accommodated by the pavement layers of specific thicknesses to prevent substantial damage to the surface. The literature is scant on the topic of load dissipation mechanisms under these unique inverted loading conditions.

To address this gap, the current study devised a comprehensive laboratory testing program aimed at evaluating the differential heave magnitudes on pavement surfaces due to the expansive nature of underlying subgrade layers. Tests were conducted across a spectrum of configurations, both unreinforced and reinforced. Specifically, four configurations were investigated: an unreinforced or control section, a section reinforced with geocells, another with geogrids, and a final one utilizing the Hybrid Geosynthetic Reinforcement System (HGRS). Subsequent sections will elaborate on the test protocols employed and the results garnered from these experiments.

3.1. Materials

3.1.1. Soil

For the experimental study, high-plasticity clay soil was selected as a subgrade to evaluate the efficacy of geosynthetics over high-swelling natural soil. The soil sample was collected from Marsing, ID which exhibited high swelling potential [4]. The soil sample was denoted as MS (for Marsing) to signify the location from which it originated. A typical poorly graded sand with gravel was used as a base course over the expansive subgrade. No asphalt layer was used in the experimental program. Standard ASTM methods were used to define the basic characteristics of the subgrade and base materials. Table 1 lists the properties of the subgrade and base materials.

3.1.2. Geocell

A high-density polyethylene (HDPE) geocell was used to evaluate the efficacy of over-swelling in the experimental study. The depth and the thickness of the geocell were 152 mm and 1.5 mm, respectively. There were 8 cells in the sample, and the expanded cell size was 370 mm by 250 mm. Table 2 illustrates the basic properties of the geocell sample.

Table 1. Geotechnical properties of the subgrade and base course used in this study along with the test specification used to determine the property.

Physical Properties	MS	Base Course	Specification
Maximum Dry Density (kg/m^3)	1095	2315	ASTM D698
Optimum Moisture Content (%)	32.5	8.5	
Gravel Content (%)	-	39.4	ASTM D6913
Sand Content (%)	4.5	59	
Silt Content (%)	19	1.6	ASTM D7928-17
Clay Content (%)	76.5	-	
Liquid Limit (%)	111	Non-plastic	ASTM D4318
Plastic Limit (%)	40	Non-plastic	
Plasticity Index (%)	71	Non-lastic	
Soil Classification	CH	SP	USCS

Table 2. Physical properties of the geocell and geogrid used in this research.

Material	Thickness (mm)	Depth (mm)	Density (kg/m^3)	Tensile Strength (MPa)	Modulus at 1% Strain (MPa)
HDPE Geocell	1.5	150	950	12.4	392

3.1.3. Geogrid

A biaxial geogrid material was used in the experimental study. This material is composed of polypropylene resin which is extruded into a grid pattern. This material is inactive to any biological process and resistant to naturally encountered chemicals, alkalis, and acids. Grid aperture size of the sample was 25.4 mm in the machine direction (MD) and 33.0 mm in the cross-machine direction (CMD). The thickness of the geogrid was 1.5 mm. Mechanical properties of the geogrid sample were found from the manufacturer which is shown in Table 3.

Table 3. Geogrid material characteristics (TenCate 2017).

Mechanical Properties	Test Method	Unit	Minimum Average Roll Value	
			MD	CMD
Tensile Strength (Ultimate)	ASTM D6637	kN/m	19.2	28.8
Tensile Strength (2% strain)	ASTM D6637	kN/m	6.0	9.0
Tensile Strength (5% strain)	ASTM D6637	kN/m	11.8	19.6
Junction Efficiency		%	93	
Flexural Stiffness		mg-cm	750,000	
Aperture Stability		m-N/deg	0.65	
Resistance to Long-term Degradation		%	100	
Resistance to UV Degradation		%	100	

3.2. Test Setup

The test setup consists of a large-scale box used to simulate a pavement section. Figure 2a illustrates a schematic of the large-scale box test setup. A transparent box made of acrylic having 12 mm wall thickness and inner dimensions of 762 mm (length) × 762 mm (width) × 762 mm (height) was used for the test setup. Garden soaker tubes were used to provide moisture to the expansive soils to ensure the maximum possible heave in the minimum possible time. This soaker system was connected to a water reservoir placed at a height of six feet above the top of the box to offer a hydraulic gradient to enhance the saturation rate of soil. External steel struts were used to support the side wall of the transparent box to make sure no lateral movement occurred due to swell pressure from the expansive soils. A grid

planer sheet was used to provide a reference plane to measure the surficial heave of the pavement surface. This sheet had 36 points arranged in a grid pattern to facilitate the heave measurements over time using a laser distance measuring tool. This tool can measure vertical distance up to 30 m with an accuracy level of 1.5 mm. A complete test setup is shown in Figure 2b.
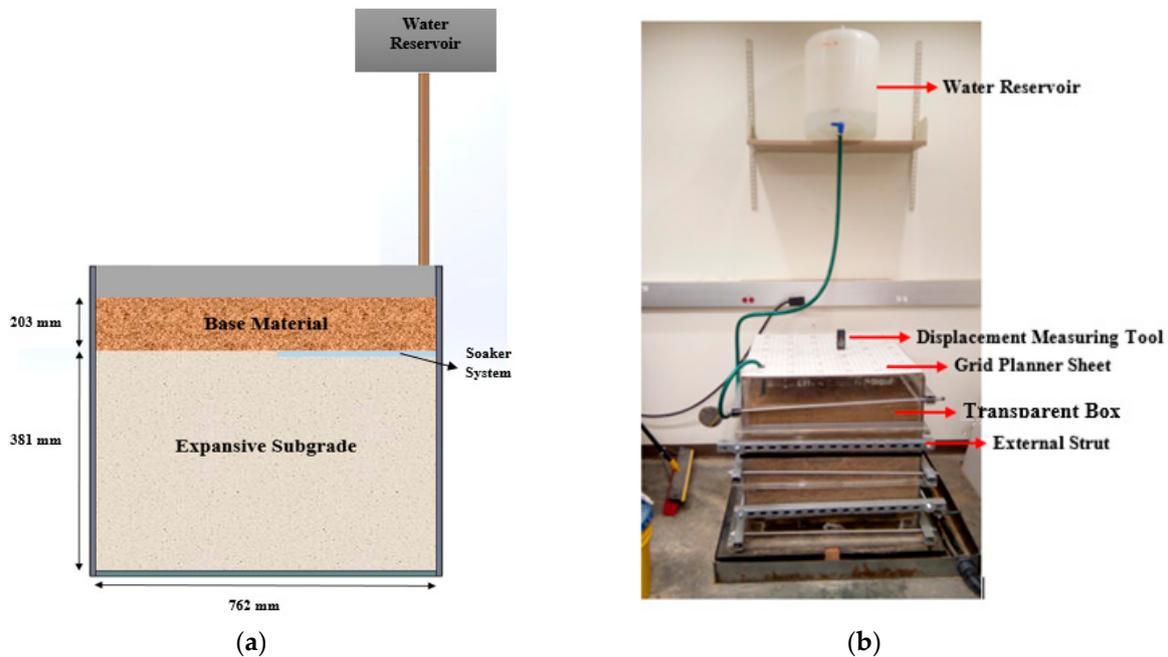
Figure 2. Experimental setup used to replicate pavement section in large box test. (**a**) Schematic and (**b**) photograph of the actual setup.

Large-scale box test comprises four configurations that include one control unreinforced section and three geosynthetic reinforced sections. These configurations are as follows:

1. Control Section (CS);
2. Geocell Reinforcement (GC);
3. Geogrid Reinforcement (GG);
4. Hybrid Geosynthetic Reinforcement System (HGRS).

Each of the test configurations and the corresponding results are discussed in the following sections. Figure 3 shows schematics of all four test configurations studied in this research.

3.2.1. Control Section (CS)

The initial test was aimed at establishing the baseline for the heave potential of the expansive soil under a pavement section resting on a conventional base layer without reinforcement. Hence, the control section without reinforcement (CS) was prepared and monitored for the differential heave on the surface. Base course and expansive subgrade (MS) samples were used for this section in the box shown in Figure 4. A 203 mm of base course material was placed over 381 mm of the expansive subgrade. The base course material was compacted at 90–95% of Maximum Dry Unit Weight (MDUW) with $6 \pm 1\%$ moisture content, and the subgrade was compacted at 95–98% of MDUW with $25 \pm 3\%$ moisture content. Hand compaction was used to compress the materials. Figure 4 shows the compaction tool for the test. Base and subgrade were compacted into four and eight layers, respectively. To ensure that the OMC and MDUW were maintained accurately the amount of soil needed for each layer was estimated based on the thickness of the layer (~50 mm for each layer) and the cross-sectional area of the box.
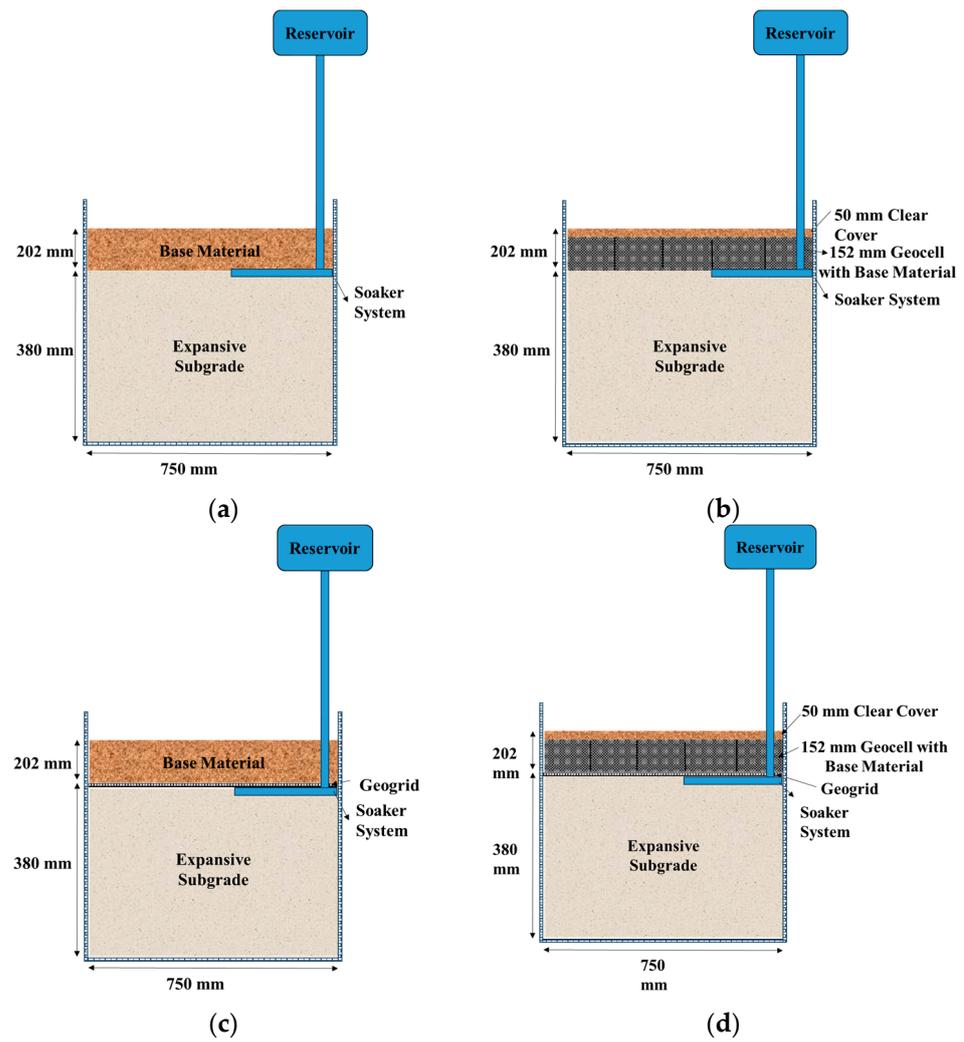
Figure 3. Schematics of test configurations. (**a**) Control Section (CS). (**b**) Geocell Reinforcement (GC). (**c**) Geogrid Reinforcement (GG). (**d**) Hybrid Geosynthetic Reinforcement System (HGRS).

Figure 4. Compacted soil and the tool used for compaction.

Soaker system arrangement was embedded at the top of the subgrade (half portion) shown in Figure 5 to initiate differential heaving. Base compaction was done in such a way that the soaker system arrangement was intact. Placement of soaker system arrangement

was selected based on several trials to find out the efficacy of the system. In these trials, soaker system was placed at the bottom, at the middle, and at the top of the subgrade and provided sufficient moisture for 15 days. In these trials, up to 101.6 mm of surficial heave was observed when the soaker system was at the top. Typically, expansive subgrades are encountered by the moisture due to surface runoff during rainfall. The water percolates through base layers into the subgrade. The soil absorbs the moisture and swells based on its swelling potential and cracks and heaves start to appear at the pavement surface. Placement of the soaker system at the top of subgrade justifies that situation. Figure 6 shows the control section after compaction. A water reservoir was connected with soaker system to provide sufficient moisture. When the complete setup was done, the outlet valve of water reservoir was opened to supply moisture which is shown in Figure 7. Initially, surrounding soils near soaker system were encountered by the moisture and it started swelling. Water was percolated through the voids and saturated the adjacent soils with time. So, differential swelling occurred within the system over time. A grid planner sheet is placed at the top of the box to provide a reference plane. Thirty-six reference points were marked on the planner sheet in a grid pattern. The vertical swelling was measured using laser displacement measuring tool as shown in Figure 8. The soil is allowed to swell for 15 days.

Figure 5. Placement of soaker system at the top half of subgrade.

**Figure 6.** Control section after compaction.

Figure 7. Moisture supply through water reservoir.

Figure 8. Measurement of vertical swelling.

3.2.2. Geocell Reinforcement (GC)

After obtaining the results from the control section, geocell was used as reinforcing material for the next test (as shown in Figure 9). HDPE geocells with 152 mm cell depth were embedded into the base course layer. Subgrade (MS) was prepared using the same process as the soaker system. Soaker system was embedded in the top half of the expansive soil section similar to the control section.
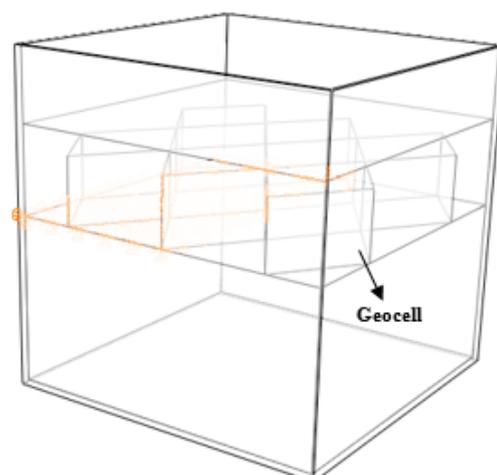
Figure 9. Schematic of GC Section.

Base course material was placed in two rounds. In the first round, geocells and base course were placed and compacted which is shown in Figure 10 and then a 51 mm of base course layer was placed as cover. Figure 11 shows the GC section after compaction. Density and water content of the soils were maintained as per control section. When the sample preparation was done, grid planner sheet was placed at the top of the box as reference plane. The water reservoir was connected to the soaker system and started the test. The test was continued for 15 days as well to compare the results with control section.
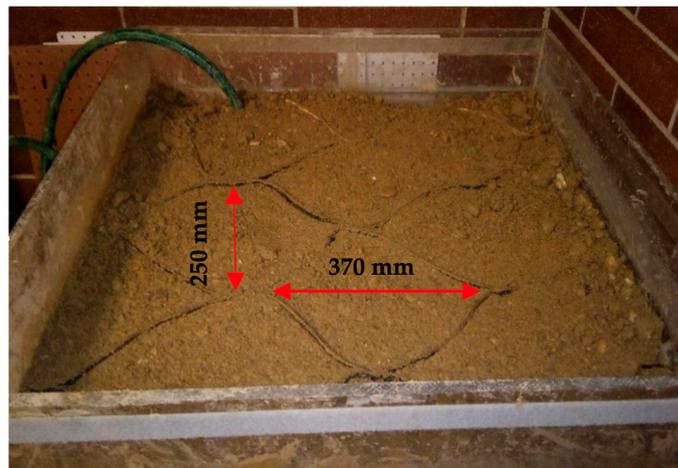
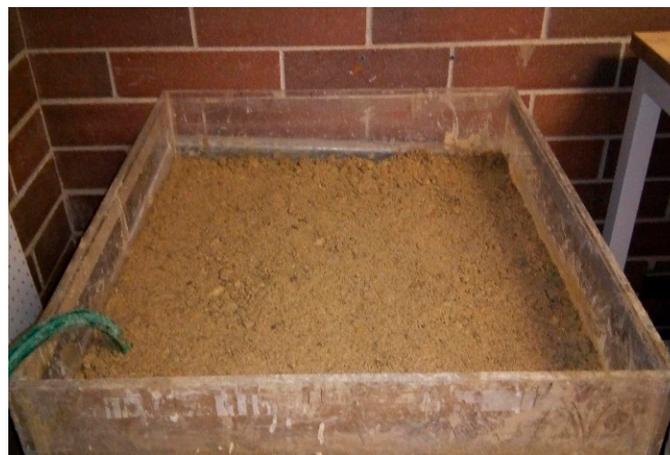**Figure 10.** Geocell placement.

Figure 11. GC section after compaction.

3.2.3. Geogrid Reinforcement (GG)

In the third test, biaxial geogrid was used to mitigate the swelling distresses in the pavement section. The pavement section with geogrid is shown in Figure 12. Geogrid is placed at the bottom layer of base as shown in Figure 13. Geogrid layer was anchored at the sides to introduce the tension effect. After compacting the subgrade according to control section, the top of subgrade and geogrid were placed above that layer.

Galvanized steel pegs were used to anchor the geogrid sheet. All the outer sides of the geogrid sheet were anchored into the soil with 5 pegs on each side with a total of 20 pegs. Figures 14 and 15 show the steel peg and geogrid anchoring into the soils, respectively. After fastening the geogrid sheet, base materials were placed and compacted as per control section. The thickness of the base and subgrade are also maintained in accordance with control section. After completing the setup, similar procedures were followed for GG section and water was provided to the subgrade for 15 days.
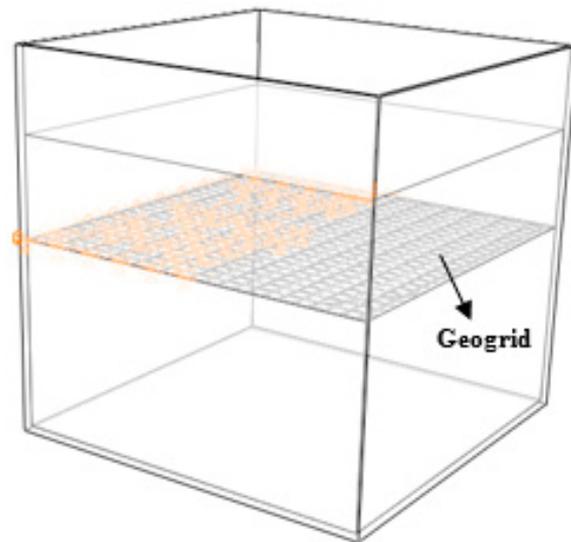
Figure 12. Schematic of GG section.


Figure 13. Geogrid placement.

Figure 14. A photograph of steel peg.

Figure 15. Anchoring geogrid using steel peg.

3.2.4. Hybrid Geosynthetic Reinforcement System

The final test of the large-scale box system was the pavement section with HGRS which is shown in Figure 16. HGRS is the combination of one geocell layer and one geogrid layer. The primary focus of this combination is to combine the advantages of geocell and geogrid in one system to dissipate swelling distress.
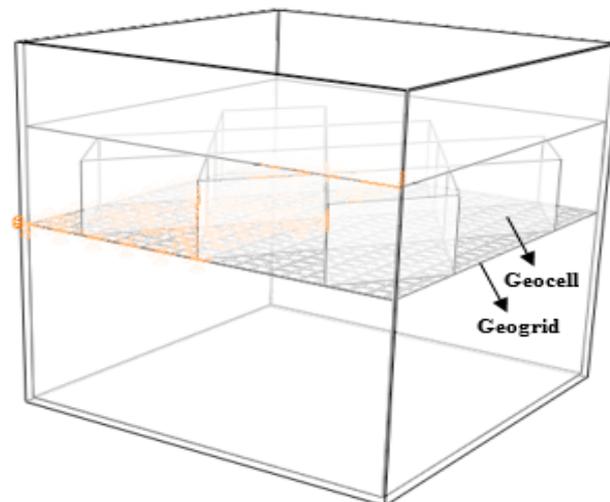
Figure 16. HGRS section.

All the procedures were the same and geocell and geogrid were placed together. After compaction of subgrade, geogrid was placed like a GG section, and 50 mm of base layer was placed at the top of geogrid and compacted for interlocking. After that, the geocell was placed in the box, filled with base course materials, and compacted. A similar process was followed like in GC section until all the cells were filled with base materials. The thickness of the base and subgrade were same as control section. Identical procedures were followed for HGRS section to provide moisture to the subgrade for up to 15 days. Figures 17 and 18 represent the geogrid and geocell installation in HGRS section, respectively.

Figure 17. Geogrid installation in HGRS section.

Figure 18. Geocell installation in HGRS section.

4. Test Results and Discussion

The main objective of the large-scale box test was to evaluate the effectiveness of HGRS to mitigate differential heave due to expansive subgrade and compare the results with the control section. The HGRS performance was also compared with GC and GG sections. Test results showed that all the reinforced systems significantly reduced the maximum heave of the pavement section compared to the control section. The performance of HGRS was dominant among the test results. Figure 19 shows the maximum heaving plot with time for all four sections tested using a large-scale box.
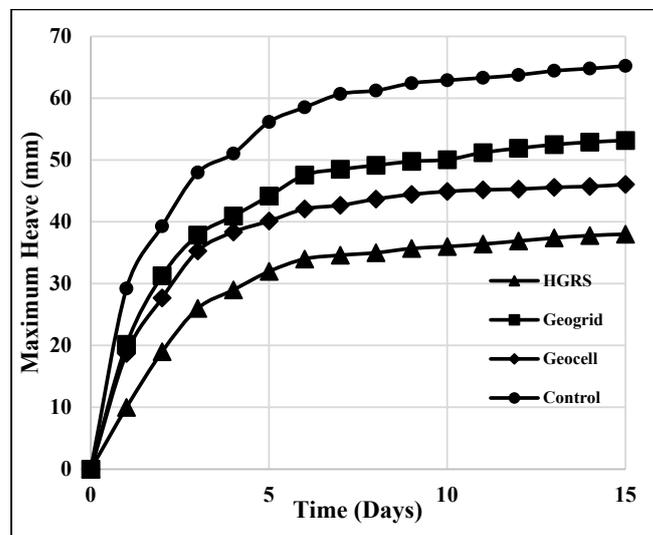

Figure 19. Maximum heaving plot over time.

It was found that the HGRS reduced the maximum surficial heave by 42% whereas geocells and geogrid reduced the maximum surficial heave by 29% and 17%, respectively. It was also revealed that the differential heave (the difference between maximum and minimum heave) on the pavement surface was also decreased considerably using the reinforcement application. HGRS application showed the highest improvement of differential heave by 62% compared to geocells (~45%) and geogrid (~31%). Test results of the large-scale box test are shown in Figure 20.
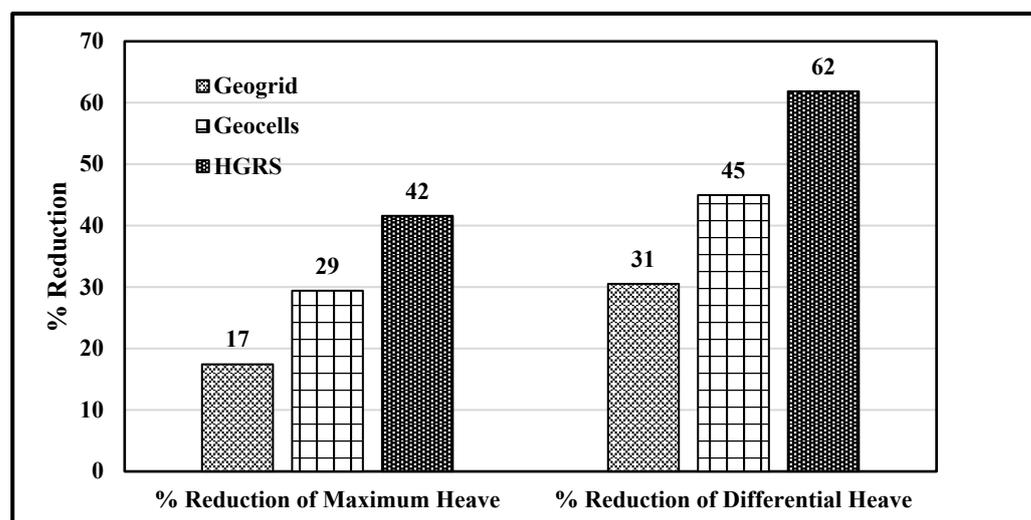

Figure 20. Comparisons of percent swell reductions for the three reinforced test sections.

5. Conclusions

This study presented comprehensive findings from a large-scale box test designed to simulate a pavement section constructed over an expansive subgrade. The box test was meticulously detailed, covering aspects such as the test setup, variables, and procedures in the "experimental program section". Through this research, several key conclusions can be gleaned regarding the use of geosynthetic systems in mitigating expansive soil-induced swelling in pavement layers.

Firstly, geosynthetic systems, particularly Hybrid Geosynthetic Reinforcement Systems (HGRS), were found to be highly effective in controlling swelling distresses on pavement surfaces. HGRS outperformed both geocells and geogrids by providing a 62% reduction in differential heave compared to the 31% and 45% of geogrids and geocells, respectively. This shows HGRS's potential as a superior alternative for soil stabilization applications.

Secondly, the incorporation of geocells in the base layer significantly enhanced the swell mitigation capability. The confinement of base course materials within the geocells contributed to the increased strength and integrity of the base layer, thereby reducing surface distress.

Thirdly, the geogrid system presented its own merits. Its interlocking and tension effects within the base layer offered basal reinforcement, effectively resisting upward soil movement and subsequently minimizing swell potential at the surface layer.

Finally, HGRS emerged as particularly effective due to its dual reinforcing mechanisms—confinement and tension. This synergy led to an increase in the stiffness of the base layer, affirming the potential of HGRS as a robust solution for mitigating soil-induced swell pressures.

In summary, the findings from this study underscore the pivotal role of geosynthetic systems, particularly HGRS, in addressing the challenges of expansive soil-induced differential heave in pavement constructions. Future work should aim to refine these systems further and explore their scalability and economic feasibility for broader civil engineering applications.

References

1. Nelson, J.D.; Chao, K.C.; Overton, D.D.; Nelson, E.J. *Foundation Engineering for Expansive Soils*; Wiley: New York, NY, USA, 2015.
2. Chen, F.H. *Foundations on Expansive Soils*, 2nd ed.; Elsevier Scientific Publishing Co., Ltd.: Amsterdam, The Netherlands, 1988.
3. Snethen, D.R.; Townsend, F.C.; Johnson, L.D.; Patrick, D.M.; Vedros, P.J. *A Review of Engineering Experiences with Expansive Soils in Highway Subgrades*; U.S. Army Engineer Waterways Experiment Station: Vicksburg, MS, USA, 1975.
4. Tamim, M. Evaluating the Effectiveness of a Hybrid Geosynthetic Reinforcement System to Mitigate Differential Heave on Flexible Pavement Due to Expansive Subgrades. Master's Thesis, Boise State University, Boise, ID, USA, 2017.
5. Al-Qadi, I.L.; Baek, J.; Buttlar, W.G. Cost-Effectiveness and Performance of Overlay Systems in Illinois. In *Guidelines for Interlayer System Selection Decision When Used in HMA Overlays*; Illinois Center for Transportation: Rantoul, IL, USA, 2009; Volume 2.
6. Nelson, J.D.; Miller, D. *Expansive Soils Problems and Practice in Foundation and Pavement Engineering*; John Wiley and Sons Inc.: Hoboken, NJ, USA, 1992.
7. Petry, T.M.; Little, D.N. Review of Stabilization of Clays and Expansive Soils in Pavements and Lightly Loaded Structures—History, Practice, and Future. *J. Mater. Civ. Eng.* **2002**, *14*, 447–460. [CrossRef]
8. Chittoori, B.C.S.; Puppala, A.J.; Wejrungsikul, T.; Hoyos, L.R. Experimental Studies on Stabilized Clays at Various Leaching Cycles. *J. Geotech. Geoenviron. Eng.* **2013**, *139*, 1665–1675. [CrossRef]
9. Islam, K.M. Subsurface Characterization of Flexible Pavements Constructed Over Expansive Soil Subgrades and Selection of Suitable Rehabilitation Alternatives. Master's Thesis, Boise State University, Boise, ID, USA, 2017.
10. Chittoori, B.; Mishra, D.; Bruce, D.; Ingram, J. Recurrent Pavement Damage from Underlying Expansive Soil Deposits: Idaho Experience. In Proceedings of the TRB 95th Annual Meeting Compendium of Papers, Washington, DC, USA, 10–14 January 2016.
11. Puppala, A.J.; Chittoori, B.; Saride, S.S. Sulfate Induced Heaving of a Taxiway: A Case Study. *Indian Geotech. J.* **2012**, *42*, 257–266. [CrossRef]
12. Perkins, S.W.; Ismeik, M. A Synthesis and Evaluation of Geosynthetic-Reinforced Base Layers in Flexible Pavements—Part I. *Geosynth. Int.* **1997**, *4*, 549–604. [CrossRef]
13. Giroud, J.-P.; Noiray, L. Geotextile-Reinforced Unpaved Road Design. *J. Geotech. Eng. Div.* **1981**, *107*, 1233–1254. [CrossRef]
14. Giroud, J.P.; Ah-Line, C.; Bonaparte, R. Design of Unpaved Roads and Trafficked Areas with Geogrids. In *Polymer Grid Reinforcement*; Amer Society of Civil Engineers: Reston, VA, USA, 1985; pp. 116–127.
15. Zornberg, J. Advances in the Use of Geosynthetics in Pavement Design. In Proceedings of the Geosynthetics India'11; IIT Madras, Chennai, India, 23–24 September 2011.
16. Cancelli, A.; Montanelli, F.; Rimoldi, P.; Zhao, A. Full Scale Laboratory Testing on Geosynthetics Reinforced Paved Roads. In Proceedings of the International Symposium on Earth Reinforcement, Fukuoka, Japan, 12–14 November 1996.
17. Haas, R.; Walls, J.; Carroll, R. Geogrid Reinforcement of Granular Bases in Flexible Pavements. *Transp. Res. Rec.* **1988**, *1188*, 19–27.
18. Halliday, A.; Potter, J. *The Performance of a Flexible Pavement Constructed on a Strong Fabric*; TRRL Laboratory Report; Transport and Road Research Laboratory (TRRL): Wokingham, UK, 1984.
19. Al-Qadi, I.; Brandon, T.; Bhutta, S. Geosynthetics Stabilized Flexible Pavements. In Proceedings of the Geosynthetics '97, Long Beach, CA, USA, 11–13 March 1997.
20. Berg, R.R. *Geosynthetic Reinforcement of the Aggregate Base/Subbase Courses of Pavement Structures*; Ryan R. Berg & Associates, Inc.: St. Paul, MN, USA, 2000.
21. Barksdale, R.D.; Brown, S.F.; Chan, F. *Potential Benefits of Geosynthetics in Flexible Pavement Systems*; Transportation Research Board: Washington, DC, USA, 1989; p. 62.
22. Webster, S.L.; Alford, S.J. *Investigation of Construction Concepts for Pavements across Soft Ground*; U.S. Army Waterways Experiment Station: Vicksburg, MS, USA, 1978.
23. Yang, X. Numerical Analyses of Geocell-Reinforced Granular Soils under Static and Repeated Loads. Ph.D. Thesis, University of Kansas, Lawrence, KS, USA, 2010.
24. Dash, S.K. Effect of Geocell Type on Load-Carrying Mechanisms of Geocell-Reinforced Sand Foundations. *Int. J. Geomech.* **2012**, *12*, 537–548. [CrossRef]
25. Han, J.; Yang, X.M.; Leshchinsky, D.; Parsons, R.L.; Rosen, A. Numerical Analysis for Mechanisms of a Geocell-Reinforced Base Under a Vertical Load. In *Geosynthetics in Civil and Environmental Engineering, Proceedings of the Geosynthetics Asia 2008 Proceedings*

of the 4th Asian Regional Conference on Geosynthetics in Shanghai, China, 17–20 June 2008; Li, G., Chen, Y., Tang, X., Eds.; Springer: Berlin/Heidelberg, Germany, 2009; pp. 741–746.

26. Saride, S.; Gowrisetti, S.; Sitharam, T.; Puppala, A.J. Numerical Simulation of Geocell-Reinforced Sand and Clay. *Proc. Inst. Civ. Eng.-Ground Improv.* **2009**, *162*, 185–198. [CrossRef]

27. Kief, O. Hybrid Geosynthetic Solution for Rail Tack on Expansive Clay. In Proceedings of the Geosynthetics 2015, Portland, OR, USA, 15–18 February 2015.

28. Yuu, J.; Han, J.; Rosen, A.; Parsons, R.; Leshchinsky, D. Technical Review of Geocell-Reinforced Base Courses over Weak Subgrade. In Proceedings of the First Pan American Geosynthetics Conference, Cancun, Mexico, 2–5 March 2008; pp. 2–5.

29. Pokharel, S.K.; Han, J.; Leshchinsky, D.; Parsons, R.L.; Halahmi, I. Behavior of Geocell-Reinforced Granular Bases under Static and Repeated Loads. In *Contemporary Topics in Ground Modification, Problem Soils, and Geo-Support*; Springer: Berlin/Heidelberg, Germany, 2009; pp. 409–416.

30. Dash, S.K.; Sireesh, S.; Sitharam, T.G. Model Studies on Circular Footing Supported on Geocell Reinforced Sand Underlain by Soft Clay. *Geotext. Geomembr.* **2003**, *21*, 197–219. [CrossRef]

31. Leshchinsky, B.; Ling, H.I. Numerical Modeling of Behavior of Railway Ballasted Structure with Geocell Confinement. *Geotext. Geomembr.* **2013**, *36*, 33–43. [CrossRef]

32. Zhou, H.; Wen, X. Model Studies on Geogrid- or Geocell-Reinforced Sand Cushion on Soft Soil. *Geotext. Geomembr.* **2008**, *26*, 231–238. [CrossRef]

33. Stienberg, M. *Geomembranes and the Control of Expansive Soils in Construction*, 1st ed.; McGraw-Hill Professional: New York, NY, USA, 1998; ISBN 978-0-07-061178-8.

34. Vessely, M.J.; Wu, J.T. Feasibility of Geosynthetic Inclusion for Reducing Swelling of Expansive Soils. *Transp. Res. Rec.* **2002**, *1787*, 42–52. [CrossRef]

35. Zornberg, J.G.; Roodi, G.H.; Ferreira, J.; Gupta, R. Monitoring Performance of Geosynthetic-Reinforced and Lime-Treated Low-Volume Roads under Traffic Loading and Environmental Conditions. In Proceedings of the GeoCongress 2012, Oakland, CA, USA, 25–29 March 2012; pp. 1310–1319.

36. Koerner, R.M. *Designing with Geosynthetics*; Xlibris Corporation: Bloomington, IN, USA, 2012; Volume 1.

37. Sitharam, T.G.; Hegde, A. Design and Construction of Geocell Foundation to Support the Embankment on Settled Red Mud. *Geotext. Geomembr.* **2013**, *41*, 55–63. [CrossRef]